European Journal of Chemistry
Journal homepage: www.eurjchem.com

Simultaneous removal of chromotrope 2B and radionuclides from mixed radioactive process wastewater using organo-bentonite

Kamal Shakir[a,*], Hussein Fouad Ghoneimy[a], Ibtisam Tadros Hennawy[b], Ahmed Faouzy Elkafrawy[c], Shokry Gad Elrab Beheir[a] and Mamdoh Refaat[a]

[a] *Nuclear Chemistry Department, Hot Laboratories Center, Atomic Energy Authority, Cairo, Nasr City, EG-13759, Egypt*
[b] *Organo-metallic and Organo-metalloid Chemistry Department, National Research Center, Cairo, Dokki, EG-12622, Egypt*
[c] *Department of Chemistry, Faculty of Science, Ain Shams University, Cairo, Abbassia, EG-11655, Egypt*

**Corresponding author at: Nuclear Chemistry Department, Hot Laboratories Center, Atomic Energy Authority, Cairo, Nasr City, EG-13759, Egypt.*
Tel.: +2.02.26340561; fax: +204.4620806. E-mail address: drkshakir@gmail.com (K. Shakir).

ARTICLE INFORMATION

Received: 30 June 2010
Received in revised form: 06 September 2010
Accepted: 29 September 2010
Online: 31 March 2011

KEYWORDS

CTAB-bentonite
Chromotrope 2B
Radionuclides
Adsorption
Radioactive wastewater
Wastewater treatment

ABSTRACT

The simultaneous removal of cationic radionuclides, ^{137}Cs(I), ^{60}Co(II) and $^{152+154}$Eu(III), and a chemically toxic anionic pollutant, the analytical reagent chromotrope 2B (C2B), from simulated mixed radioactive process wastewater (MRPWW) has been investigated using bentonite modified with cetyltrimethylammonium bromide. Modification was confirmed by elemental analysis, X-ray diffraction and infrared spectroscopy. Bentonite partially modified to 78% of the cation exchange capacity (PMB) was found capable to adsorb adequately both C2B and the radionuclides from aqueous solutions. Detailed batch kinetics and isotherm studies for removal of C2B singly and the radionuclides simultaneously were performed. The C2B and radionuclides kinetics conform to pseudo-first-order rate equation and the adsorption isotherms are treated with Freundlich and Langmuir models. Thermodynamic parameters were evaluated. Results suggest physisorption and ion-exchange as the principal uptake mechanism for C2B and the radionuclides, respectively. High simultaneous removal was obtained for C2B (≈ 100%) and each of the test radionuclides (>99%) from the simulated MRPWW.

1. Introduction

The nuclear industry, radiochemical and isotope production laboratories and all users of radioactive materials produce a wide range of liquid wastes and lots of wastewater of different qualities and radioactivity levels. Such wastes often need to be treated before being discharged into the environment. Of these wastes radioactive process wastewater (RPWW) is ordinarily produced at high rates. It is a dilute solution usually consisting of ordinary drinking water having a very low radioactivity level and containing small amounts of inorganic and organic laboratory chemicals [1,2]. In most cases, treatment of this water is concerned with removal of radionuclides only and other harmful pollutants are neglected though, from a safety point of view, it is of major importance to remove the harmful pollutants as well. Because of very low concentrations, the radionuclides cannot be removed by the currently used drinking water purification techniques (chemical precipitation and flocculation). Also, other separation techniques including ion-exchange and reverse osmosis are not recommended since they are either time consuming or expensive or both [1]. In our laboratory, considerable effort has been devoted to develop methods for removal of radionuclides from radioactive process wastewater [1-6]. The studies have now been extended to treatment of mixed radioactive process wastewater (MRPWW) that is radioactive process wastewater which, in addition to being radioactive, contains chemically harmful contaminants. In this regard, all the investigations so far published in the literature on removal of radionuclides and toxic organics from aqueous solutions have dealt with removal of either singly. Therefore, effective technological processes are essentially required for simultaneous once-through removal of both types.

The present paper is concerned with treatment of mixed radioactive process wastewater simulated to that possibly generated by radiochemical laboratories of the Hot Laboratories Center at Inshas, Egypt. The solution contained, in addition to radionuclides, the toxic anionic analytical reagent chromotrope 2B (C2B) and other organic and inorganic contaminants of varying chemical property. The tested radionulides were ^{137}Cs(I), ^{60}Co(II) and $^{152+154}$Eu(III). These radionuclides were selected on the grounds that: (*i*) ^{137}Cs(I) and ^{60}Co(II) are frequently encountered in radioactive waste solutions and are extremely hazardous because of their relatively high energy (both are hard γ-emitters) and long half-lives (30.1 and 5.27 years, respectively); (*ii*) the selected metals are representative of a wide range of chemical properties by including the alkali metal Cs, the transition metal Co and the rare earth metal Eu; and (*iii*) the selected metals exemplify monovalent, bivalent and trivalent metal cations.

The other pollutant, chromotrope 2B, acid red 176, (C2B), is an anionic water soluble azo dye. Azo dyes are widely used not only in textile industries but also in many other applications involving analytical purposes [7,8]. C2B is used in analytical and radiochemical laboratories for determination of various metal ions, e.g. Th, Sc, Y, La [7,9,10], organic compounds and pharmaceutical products [11] and in biological and biomedical research laboratories as a stain [12]. Hence,

ISSN 2153-2249 (Print) / ISSN 2153-2257 (Online) © 2011 EURJCHEM
DOI:10.5155/eurjchem.2.1.83-93.191

chromotrope 2B-bearing wastewaters are discharged as a result of those activities beside dyestuff manufacturing processes.

Colored waters are aesthetically objectionable for drinking, irrigation, industrial applications and other purposes. Furthermore, many dyes, especially those containing azo aromatic groups such as chromotrope 2B, are toxic, carcinogenic and mutagenic [13]. They resist biological, chemical and photochemical degradation [14]. Therefore, removal of C2B from wastewater before it is discharged into the natural water bodies is as important as radionuclides removal. The conventional approach to treat water contaminated with pollutants of different types (organic/ inorganic) and charge sign has been to study removal of each contaminant independently, mostly using different types of separation processes. The major short-comings of conventional treatment include high cost, long treatment processing and costly safe disposal of toxic secondary wastes. Hence, removal of different types of contaminants simultaneously by a single separation process, if possible, would offer obvious treatment and economic advantages. So far, this possibility has not been addressed by the researchers, and no papers are found in the literature on simultaneous removal of cationic radionuclides and anionic organics. Therefore, the objective of this study was focused on finding an appropriate process for simultaneous removal of both types of contaminants from the mixed radioactive process wastewater under test.

Of the various methods applicable for removal of radionuclides, dyes and other pollutants from wastewater, adsorption has proved to be very effective. Bentonite has been considered as one of the appropriate low-cost adsorbents for treating polluted water. Bentonite can effectively sorb various cationic organic [15] and inorganic pollutants such as heavy metals [16] and radionuclides [17] from aqueous solutions. Bentonite is mainly composed of montmorillonite, which is a 2:1 type layer consisting of one octahedral sheet of alumina inserted in between two silica tetrahedral sheets. Substitutions within the lattice structure of trivalent aluminum for quadrivalent silicon in the tetrahedral sheet and of cations of lower valence, especially Mg^{2+} or Zn^{2+} for trivalent aluminum in the octahedral sheet result in a net negative charge on the clay surfaces [18]. Interlayer cations, such as H^+, Na^+ or Ca^{2+}, balance the total electrostatic charge. Under these conditions of diminished interlayer attraction, water can interleave between layers rendering each triple layer surface equivalent to an exterior one, and the balancing interlayer ions can exchange [19]. Replacement of inorganic cations by long-chain quarter-nary ammonium cations (LQAC), such as cetyltrimethyl ammonium bromide (CTAB), converts the surface of the clay from hydrophilic (due to strong hydration of inorganic cations), to hydrophobic. Initially, sorption of LQAC onto clay takes place via cation-exchange reactions in the interlayer causing extensive clay aggregation [20]. As the loading is increased, the surfactant adsorbs to the external surfaces of aggregates via both cation-exchange and hydrophobic bonding. The latter results in building of positive charge on the clay surfaces exposed to the bulk solution [20-25] causing organoclay disaggregation [20]. Consequently, organophilic clays are highly effective sorbents for aqueous phase non-ionic organics as well as anionic organic and inorganic pollutants. Many investigations are found in the literature on the adsorption of anionic dyes by organobentonite, but none of them has examined adsorption of chromotrope 2B. Previous studies indicated that it is possible to use clays partially modified with quaternary ammonium ions as adsorbents for pollutants of different charge sign. Nevertheless, investigations for simultaneous sorption of cationic metal ions or radionuclides and anionic organic contaminants, including dyes, are so far lacking in the literature. To the best of our knowledge, this is the first report where surfactant-modified clay is used for mixed anionic organic/cationic metal ions or radionuclides removal from water.

The aim of the present work was, therefore, to explore the effectiveness of bentonite partially modified with the cationic surfactant cetyltrimethylammonium bromide (CTAB) for simultaneous removal of harmful pollutants from mixed radioactive process wastewater contaminated with a harmful chemical anionic pollutant (chromotrope 2B (C2B)) and radioactive pollutants (^{137}Cs(I), ^{60}Co(II) and $^{152+154}$Eu(III)). For this purpose sorptions of C2B and radionuclides by PMB were first investigated using pure aqueous solutions of the sorbates. Batch kinetics and isotherm studies were conducted to evaluate the adsorption efficiency of PMB. Also, the effects of process variables such as contact time, pH, and sorption efficiency were investigated and the removal conditions were optimized. The potential use of the PMB to treat the MRPWW was then investigated.

2. Experimental

2.1. Materials

Chromotrope 2B (acid red 176, C.I. 16575, molecular weight = 469.37) (denoted C2B) is 3-(*p*-nitrophenylazo)-chromotropic acid. It is an anionic monoazo acid dye obtained from B.D.H. Its structure is illustrated in Figure 1.

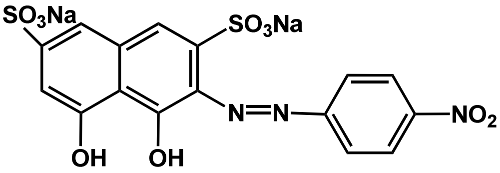

Figure 1. Chemical structure of C2B.

The isotopes ^{137}Cs(I), ^{60}Co(II) and $^{152+154}$Eu(III) were used as tracers. ^{137}Cs(I) was obtained from the Radiochemical Center, Amersham, England in the form of its chloride. ^{60}Co(II) and $^{152+154}$Eu(III) were prepared by irradiating cobalt chloride and high purity grade europium oxide in the Egyptian Second Research Reactor at Inshas, Egypt.

Spiked standard stock solutions of Cs(I), Co(II) and Eu(III) chloride were prepared separately by dissolving the calculated amount of metal salt in double distilled water, adding a known volume of the solution of the corresponding tracer and making the volume to the mark with double distilled water.

The surfactant used to modify the bentonite was the cationic surfactant cetyltrimethylammonium bromide (CTAB) with purity 99% and was purchased from Aldrich Chemical Co.

Bentonite used in this work is exploited from Kasr El Sagha, Fayoum, Egypt. It is commercially available at low cost. The natural bentonite (NB) was gently crushed, ground in a rod mill (closed circuit) and then sieved. The 53 μm fraction was oven-heated at 85 °C for 3 h and finally dried for 1 h at 105 °C and was used without any further treatment.

Capacity of PMB to remove simultaneously C2B and radionuclides from MRPWW was investigated using a solution simulated the MRPWW possibly generated by radiochemical laboratories of the Hot Laboratories Center at Inshas. The solution was prepared by dissolving, in tap water, calculated volumes of standard solutions of C2B, metal chlorides spiked with the respective radionuclide(s) ^{137}Cs(I), ^{60}Co(II) and/or $^{152+154}$Eu(III) and other desired organic and inorganic laboratory chemicals. The chemical composition of tap water and the simulated mixed radioactive process wastewater (MRPWW) are given in Table 1.

Table 1. Composition of tap water and the simulated MRPWW.

Water type	**Composition**								
Tap water (pH ~7.1)	**Ion**	**Ca^{2+}**	**Mg^{2+}**	**Na^{+}**	**K^{+}**	**Fe^{3+}**	**Cl^{-}**	**SO_4^{2-}**	**ΣCO_2***
	Conc. (mg L^{-1})	32	18	34	5.5	0.1	4	58	158.5
MRPWW	Tap water containing $1x10^{-4}$M C2B; ^{137}Cs(I), ^{60}Co(II), $^{152+154}$Eu(III) ($1x10^{-6}$ M of each); HDEHP, TBP, *n*-hexane, EDTA (2 μg/L of each); Zn^{2+}, PO_4^{3-} (1 μg/L of each), pH 7.0-7.3								

* $\sum CO_2 = HCO_3^- + CO_3^{2-} + CO_2$; HDEHP = di-2-ethylhexyl phosphoric acid; TBP = tributyl phosphate; EDTA = ethylenediaminetetraacetic acid.

2.2. Organobentonite synthesis

The partially modified bentonite (PMB) was synthesized by adding the calculated weight of the dried bentonite to 250 mL of double distilled water containing the mass of CTAB needed to achieve the desired percentage of the clay's CEC. The suspension was then shaken, at 65 °C, for 4 h. The treated clay was left over-night to settle and the supernatant solution was separated by decantation. The treated clay was then washed by shaking with 250 mL of double distilled water for 1 h, left to settle and then separated. The washing process was repeated several times until the washings were free from bromide ions as indicated by $AgNO_3$. The organo-bentonite was at last separated from water by vacuum filtration, dried at 80 °C, activated for 1 h at 105 °C, and gently ground with a mortar and pestle to break up aggregate particles.

2.3. Apparatus

The chemical analysis of natural bentonite (NB) was carried out by X-Ray fluorescence (Axios, sequential WD-XRF spectrophotometer, PANalytical 2005). The elemental analysis of NB and PMB was carried out in the Analytical Services Unit at the National Research Center, using Vario Elementar CHN analyzer. The X-ray powder diffraction (XRD) patterns of NB and PMB were obtained using Shimadzu Diffractometer (XRD-DI series) using a nickel–filter and CuK_α radiation source (λ = 0.154 nm) at 40 kV and 30 mA. XRD patterns were obtained between 2° and 90° 2θ with a scan speed and step size of 1°/min and 0.02°, respectively. Spectra of infrared absorption (IR) for NB and PMB were recorded in the range between 4000 and 500 cm^{-1} with 4 cm^{-1} resolution using Pomen, Hartman spectrophotometer to confirm surface modification of bentonite. An Ortec Coaxial High Purity Ge detector connected to a multichannel analyzer model GEM-100210-P-Plus of 8192 channel was used for radioactivity measurements of the radionuclides.

2.4. Sorption experiments

Sorption studies were carried out by shaking, for appropriate time intervals, 0.25 g of adsorbent with 25 mL of adsorbate(s) solution of the desired concentration (C2B = $1x10^{-4}$ M; radionuclide = $1x10^{-6}$ M unless otherwise specified) and pH adjusted with analytical grade HCl or NaOH solution. The temperature was kept constant at 30±1 °C, unless otherwise stated. Shaking was carried out in a temperature-controlled water bath shaker (Karl Kolb type, D-6072 Dreieich, Germany). After equilibration, the solution and solid phases were separated from each other by centrifugation at a speed of 5000 rpm using Chirana centrifuge. The residual dye concentration was spectrophotometrically estimated in the supernatant solution by monitoring the color absorbance before and after adsorption. Each experiment was performed twice or more under identical experimental conditions.

Effects of different operating factors on sorption of the radionuclides were investigated using a triple-solute solution $1x10^{-6}$ M in each of Cs(I), Co(II) and Eu(III). Experiments for simultaneous removal of C2B and radionuclides were performed using multisolute solution $1x10^{-4}$ M in C2B and $1x10^{-6}$ M in each of the three concerned metal cations.

2.5. Analytical methods

The cation exchange capacity (CEC) of bentonite was determined by the methylene blue-acid titration method [26] and has been found to be 679 mmol/kg of bentonite.

The amount of CTAB sorbed to bentonite was determined by two methods: (*i*) from the results of the organic carbon content and (*ii*) as the difference between the initial and final amount of CTAB in solution used to modify bentonite as determined spectrophotometrically by the bromothymol blue method [27].

C2B concentration in solution was determined spectrophotometrically at λ_{max} of 520 nm using UV-Vis spectrophotometer (Bausch & Lomb spectrophotometer). Experiments have shown that ions which might dissolve from the adsorbent in the pH range used in this study do not affect the color intensity. Also, it was found that the absorbance of C2B is not affected by the pH in the range 4.5-6.5. Depending on its concentration, CTAB affects the absorbance of C2B up to concentration of about $6x10^{-4}$ M CTAB beyond which the absorbance becomes almost constant. Hence, the analysis of C2B was carried out at pH 5.4 ± 0.2 in presence of 0.002M CTAB.

The adsorption percent and the amount of dye adsorbed (q_t) in mmol/g of PMB were determined using the relationships:

$$Adsorption\% = \frac{C_o - C_t}{C_o}\ x\ 100\ \text{, and} \qquad (1)$$

$$q_t = (C_o - C_t)\,\frac{V}{m} \qquad (2)$$

Where C_o (mmol/L) is the initial concentration of the dye; C_t (mmol/L) is the concentration of the dye in the solution at time t; *V* is the volume of the solution (L) and *m* is the mass of the adsorbent (g). Sorption of radionuclides on PMB was determined radiometrically in terms of percentage adsorption.

3. Results and discussion

3.1. Natural and modified bentonite characterization

The chemical composition of NB, determined by XRF analysis showed that silica and alumina are the major constituents of the clay along with iron oxides which are present at lower quantities. In addition, various metal oxides are present at much lower amounts. Consequently adsorbates will be, expectedly, removed by silica and/or alumina, and possibly by iron oxides.

The organic C content of the natural clay was found nil in comparison to the synthesized organoclay. Hence the organic C in PMB was entirely derived from the exchanged CTAB cations, suggesting intercalation of CTAB molecules between the bentonite layers. Intercalation of CTAB was confirmed by the C/N ratio determined for modified bentonite from elemental analysis and the theoretically calculated C/N ratio for CTAB which have been found comparable.

Intercalation of CTAB cations between interlayers of bentonite was further confirmed by XRD measurements (Figure 2a) which generally reveal that the intercalation process is accompanied by expansion of the interlamellar spacing of the bentonite. As seen in Figure 2a, the XRD patterns of NB show basal spacing (d-spacing) of 1.5 Å at about 62.5° (2θ) indicating the presence of both Na^+ and Ca^{2+} as interlayer cations [28]. On treatment with CTAB the silicate layers became saturated with a mixture of Na^+, Ca^{2+} and CTAB cations and the basal spacing (d_{001}) increased from 16.23 Å for NB to 19.24 Å for PMB (Figure 2a). This change in basal spacing corresponds to a bilayer of organic cations between the silicate layers [29].

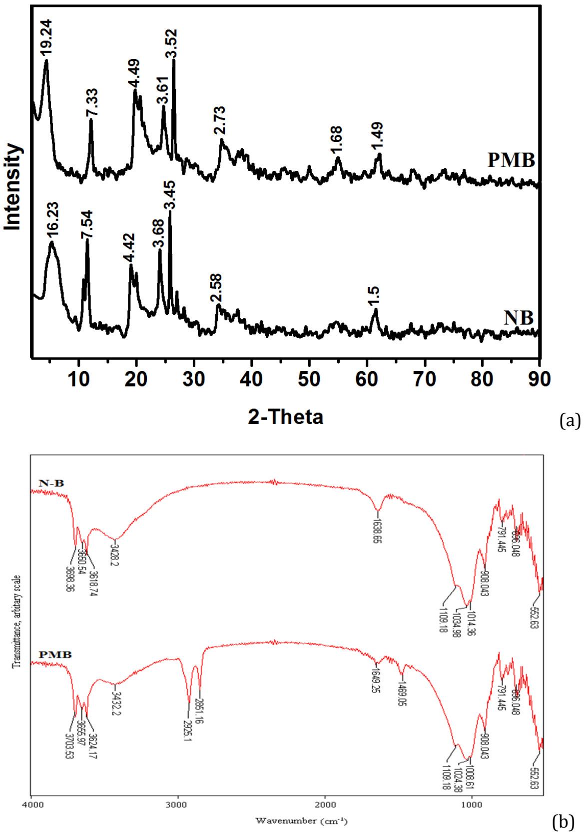

Figure 2. XRD (A) and FT-IR (B) spectra of NB and PMB.

Additional evidences for intercalation of CTAB cations into the silicate lattice of the bentonite were obtained by comparing the FT-IR spectra of the derived organobentonite to those of NB (Figure 2b). As seen in the figure, the peak intensity of H-O-H stretching (3432 cm^{-1}) and H-O-H bending (1649 cm^{-1}) for the modified bentonite are lower than those of the NB, 3428 cm^{-1} and 1638 cm^{-1}, respectively. Also, the absorption peak at 1469 cm^{-1} in modified bentonite (Figure 2b), which is related to bending vibrations of NH_4^+ and their bonding, clearly indicates surface modification of NB by CTAB cation. Further evidence for the intercalation of $[CTA]^+$ cations between silica layers of the bentonite is shown by the presence of the strong absorption bands at 2925 and 2851 cm^{-1} for only modified bentonite, which correspond to the symmetric and asymmetric stretching vibrations of the methylene groups [30] of the aliphatic chain of CTAB.

3.2. Effect of incorporated CTAB quantity on adsorption properties of bentonite

Generally, modification of bentonite results in substantial improvement of its sorption capability for organic and inorganic anions and non-ionic organics but its sorption ability for cationic species is considerably decreased. However, this drawback can be overcome by partially modifying the bentonite [28,31,32]. Therefore, it was necessary to determine the optimal concentration of CTAB required synthesizing partially modified bentonite which possess the maximum possible sorption capacity for an anionic pollutant and can simultaneously effectively remove cationic contaminants. For those purposes, the effect of CTAB content in modified bentonite on its efficiency for adsorption of C2B and radionuclides from aqueous solutions was investigated.

As expected, Figure 3 reveals that sorption of the anionic dye (C2B) increases whereas sorptions of the cations Cs(I), Co(II) and Eu(III) decrease with increasing $[CTA]^+$ cation incorporation indicating that presorbed cationic surfactant blocked sorption sites for metal cations. When modification to 70-80% of the CEC was reached, the organoclay was capable to sorb both the anionic and cationic pollutants in acceptable amounts. Bentonite modified with CTAB to 78% of its CEC was selected for use in further experimental work.

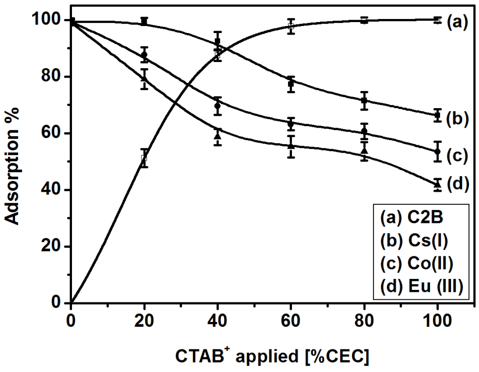

Figure 3. Variation of the quantity of dye and radionuclides sorbed with the percentage of CTAB exchanged in the clay. Conditions: C2B conc. = $1x10^{-4}$ M; Radionuclide conc. = $1x10^{-6}$ M; PMB mass = 10 g/L; pH = 7.5; Temp. = 30±1°C; Shaking time = 3h.

3.3. Effect of contact time

3.3.1. Sorption of C2B

Figure 4a shows the effect of contact time on uptake of $1x10^{-4}$ M C2B onto PMB at various values of pH. The maximum percentage uptake of the dye is independent of the pH, where at all studied pH values, pH = 5.2, 8.1 and 11.2 (Figure 4a) and pH 2.5-12.7 as will be seen when the effect of pH is discussed, it approached 100%. On the other hand, the equilibrium time strongly depends on the pH. It decreased from about 100 min to 7 min as the pH was increased from 5.2 to 11.2. Figure 4a (right-insert) shows that the amount of C2B adsorbed at equilibrium increased from 0.0099 mmol/g to 0.0415 mmol/g adsorbent as the initial C2B concentration was increased from 0.1 mmol/L to 0.6 mmol/L, due to increase in the mass driving force which enforces more C2B to diffuse from the bulk solution to the adsorbent surface at a given time [25]. On the contrary, the percentage adsorption of C2B onto PMB increased from about 69.2% to 99.9% as the initial C2B concentration was decreased from 0.6 mmol/L to 0.1 mmol/L. This observed increase in the percentage adsorption is attributed to the availability of larger sorbent surface sites for relatively small amount of the adsorbate at the lower concentration [25].

3.3.2. Sorption of radionuclides

The results of the effect of contact time on simultaneous sorption of the three concerned radionuclides from triple-solute solutions of pH = 7.4 and $1x10^{-6}$ M in each of Cs(I), Co(II) and Eu(III) are presented in Figure 4b. As shown, sorption increased with increase in time and became constant after 120, 110 and 90 minutes for Cs(I), Co(II) and Eu(III), respectively. A time period of 180 minutes was chosen for sorption studies of the radionuclides.

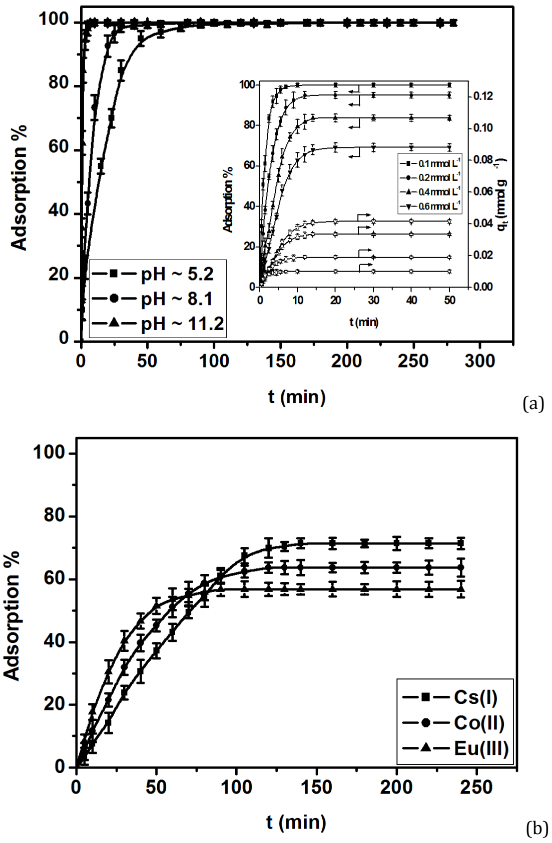

Figure 4. Sorption kinetics of C2B and the radionuclides onto PMB. (a) Effect of contact time on adsorption of C2B at different pH values and various initial C2B concentrations (right-insert); (b) Effect of contact time on sorption of radionuclides at pH ~ 7.4. Conditions: C2B conc. = 1x10^{-4} M; radionuclide conc. = 1x10^{-6} M; PMB mass = 10 g/L; temp. = 30 ± 1°C.

3.4. Effect of pH and ionic strength

3.4.1. Sorption of C2B

To study the effect of pH on the percentage removal of C2B by NB and PMB, experiments were carried out using solutions of various pH values in the range 1.2-12.7 (adjusted with HCl or NaOH), a constant dye concentration (1x10^{-4} M), fixed adsorbent mass (0.25 g) and constant volume of solution (25 mL). Results obtained are depicted in Figure 5a. In the same figure is also shown, for comparison, the theoretical dye adsorption-pH curve that is the dye dissociation-pH curve. This curve was theoretically calculated from published dissociation constants of the dye (pK values 3.86, 6.8, 9.3 and 9.86 [33]) assuming that the dissociation products were completely removed from the solution by adsorption as soon as they were formed. As shown in Figure 5a (curve a), the calculated adsorption curve shows that at pH = 2.1 the dissociation starts to increase sharply with pH elevation. At lower values of pH the dissociation is insignificant (< 1.71%) and the dye exists mainly as the protonated (non-charged) molecule. At and above pH = 5.8 only an insignificant fraction of the dye remains in the neutral form.

Figure 5a (curve b) shows that NB has little affinity for C2B. The removal capability strongly depends on the pH of solution. Maximum removal was achieved at the most acidic pH value tested where the neutral C2B molecule predominates (Figure 5a curve a) and decreased on further elevation in the pH of solution. Bentonite used in the present work is mainly constituted of oxides, primarily those of silicon, aluminium and iron. In aqueous solution, these oxides tend to form hydroxide complexes which can be protonated or deprotonated by adsorption of H^+ and OH^- respectively [34]. Hence, the developed surface charge strongly depends on the pH. At low pH, a positively charged surface prevails and at high pH a negatively charged surface is formed. At some intermediate pH (the isoelectric point) the net surface charge will be zero. The isoelectric point of silica, iron oxide and alumina are: 2±0.2, 6.7±0.2 and 8.0±0.2, respectively [35]. Referring to Figure 5a (curve b), it is seen that maximum removal by NB was achieved at the most acidic pH value tested, pH < 1.5, and decreased as the pH was increased. In acidic pH both the dye and the three major metal oxides present in the bentonite are protonated. Consequently the neutral dye molecule predominates in solution while the number of positively charged sites on the surface of bentonite increases forming exchange sites for the dye whether it is present in anionic or molecular form [36]. As a result, maximum removal of the dye is achieved at acid pH. On the other hand, when the pH of the system was increased, the removal capacity of natural bentonite decreased due to increase in the number of negatively charged sites on the clay.

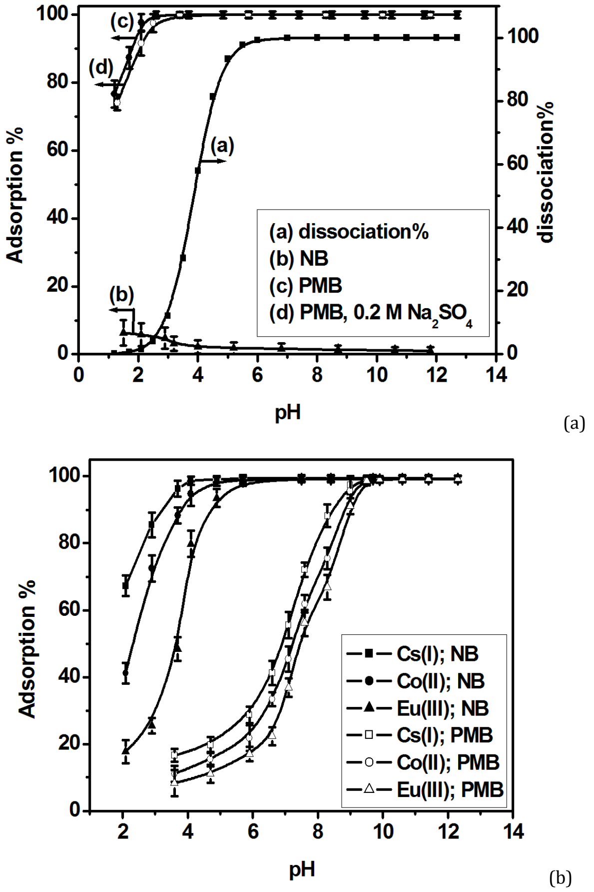

Figure 5. Effect of pH on C2B dissociation and on sorption of 1x10^{-4} M C2B onto PMB (a) and on the radionuclides uptake onto NB and PMB (b). Conditions: C2B conc. = 1x10^{-4} M; radionuclide conc. = 1x10^{-6} M; PMB mass = 10 g/L; temp. = 30±1°C.

In contrast to NB, PMB shows strong affinity for C2B. Obviously, electrostatic interactions between anionic dye molecule and the positively charged surface of the adsorbent are involved in the dye uptake. Being strongly ionized, the dissociation of the clay modifier, CTAB, does not significantly depend on the pH of solution. Hence, the magnitude of the positive charge on the organoclay is unaffected by pH-change and the effect of pH would be, therefore, due to its alteration of the dye speciation. As shown from Figure 5a (curve c), removals approaching 100% were achieved at about pH = 2.5 and above. At pH ≥ 1.2 the dye starts dissociation (Figure 5a curve a), hence removals at pH ≥ 2.5 may be attributed to electrostatic attraction between formed anionic dye species and positively charged sites on the adsorbent. However, the extent of adsorption obtained experimentally at a given pH in the lower pH region (Figure 5a curve c) is seen to be considerably higher than theoretically predicted (Figure 5a curve a). This observed increase in experimental adsorption may be attributed to simultaneous equilibria between dissociated and undissociated dye species, thus, removal of the dissociation products from the solution (ca. by adsorption) accelerates dissociation as a consequence of the simultaneous equilibria which in turn results in increase in adsorption [4].

Considering that electrostatic interaction is very sensitive to ionic strength and it decreases with its increase [37], which is not the case as shown on comparing the efficiency of adsorption of C2B at pH values > 2.5 from pure dye solution (Figure 5a, curve c) to that from 0.2M Na_2SO_4 solution (Figure 5a, curve d); it can be concluded that electrostatic attraction is not the sole sorption mechanism under the experimental conditions. Because hydrophobic attraction is known to be insensitive, or it even increases with increase in ionic strength due to the "salting out effect" [38]; it is suggested that beside electrostatic interaction, hydrophobic attraction plays a significant role in adsorption of C2B onto PMB.

3.4.2. Sorption of radionuclides

As shown from Figure 5b, the percentage sorption of the radionuclides increase markedly with increasing pH up to about pH = 7.5 and 9.5 for sorption onto NB and PMB, respectively where sorption > 99% is achieved. Beyond pH = 7.5 and 9.5 sorption approaching 100% is attained and does not change with time. Sorption of the radionuclides is primarily influenced by the surface charge on the sorbent which, in turn, is influenced by the solution pH. As discussed above, at low pH values the sorbent (NB or PMB) surface is positively charged hence it cannot sorb the similarly charged radionuclides. As the pH value of the solution is increased the positive charge on the sorbent surface decreases and the number of negatively charged sites increases causing increase in radionuclide sorption.

3.5. Isotherm studies

3.5.1. Sorption of C2B

Figure 6a-b shows the adsorption isotherms of C2B onto PMB at pH=~11.2 and temperatures of 30, 40 and 50±1 °C. From this figure it can be observed that the maximum amount of C2B adsorbed onto PMB at equilibrium decreased from 0.0947 mmol/g to 0.0902 mmol/g as the temperature was increased from 30 to 50 °C. This decrease indicates that the adsorption of C2B onto PMB favors low temperature which indicates that the adsorption process is exothermic in nature.

The equilibrium data for adsorption of C2B onto PMB were then analyzed by the linear forms of the Freundlich and Langmuir models; Eq. (3) and (4), respectively.

$$\log q_e = \log K_F + \frac{1}{n}\log C_e \tag{3}$$

$$\frac{C_e}{q_e} = \frac{1}{q_{max}\ K_L} + \frac{C_e}{q_{max}} \tag{4}$$

Where q_e is the amount of solute adsorbed per gram of PMB at equilibrium; C_e is its concentration remaining in the solution at equilibrium (mmol/L); K_F and $1/n$ are positive valued adjusttable parameters that can be related to the strength of the adsorption bond and bond distribution, respectively. As $1/n$ approaches 0, surface site heterogeneity increases, indicating that there is a broad distribution of adsorption site types. Conversely, as $1/n$ approaches unity, surface site homogeneity increases, indicating that there is a narrow distribution of adsorption site types. q_{max} is the adsorption maximum or what is generally termed the monolayer capacity and has the units of q_e (mmol/g); and K_L is a constant related to the intensity of adsorption (L/mmol).

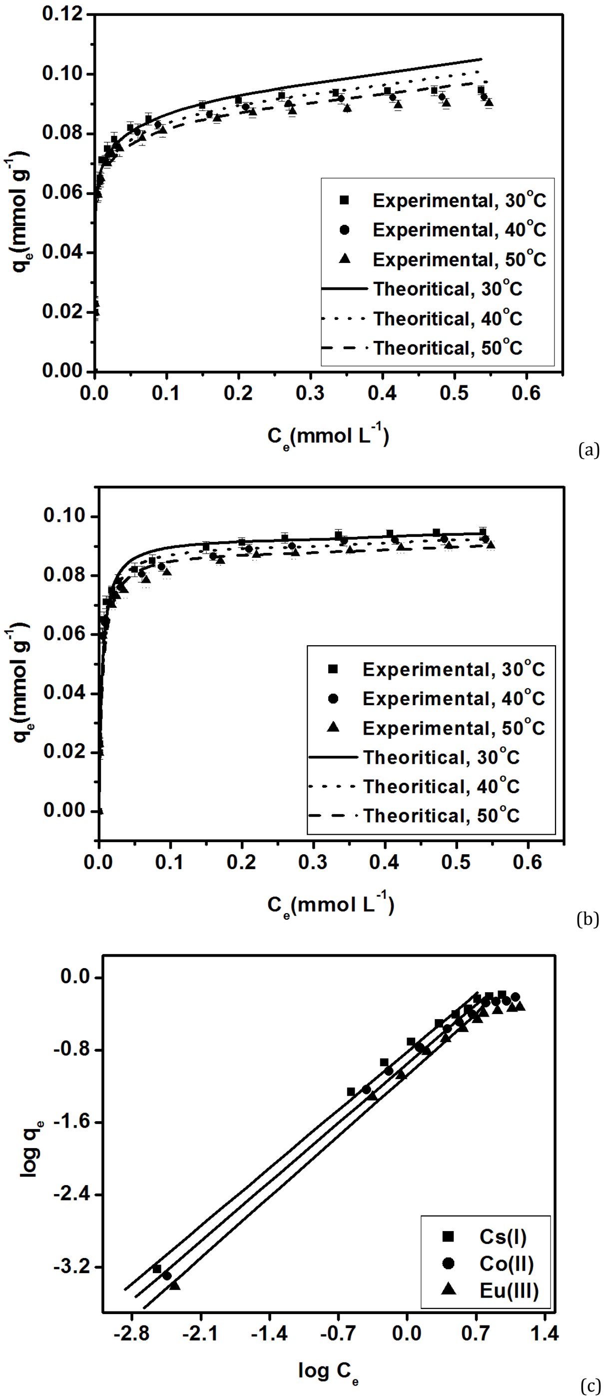

Figure 6. Sorption isotherms for C2B and radionuclides onto PMB. (a) Experimental results for C2B and calculated Freundlich isotherms, (b) Experimental results for C2B and calculated Langmuir isotherms, (c) Freundlich isotherms for the radionuclides. Conditions: PMB mass = 10 g/L; shaking time = 3 h.

Table 2. Isotherm parameters for adsorption of C2B onto PMB.

Adsorption isotherm and parameters of C2B		Temperature		
		30 °C	**40 °C**	**50 °C**
Freundlich	1/n	0.102 ± 0.0075	0.100 3 ± 0.006	0.0953 ± 0.004
	K_F	0.1093 ± 0.012	0.105 ± 0.0095	0.101 ± 0.0061
	r_F^2	0.9788	0.9841	0.9923
Langmuir	q_{max} (mmol/g)	0.0943 ± 0.0035	0.0918 ± 0.0027	0.0901 ± 0.0021
	K_L (L/mmol)	226.12 ± 0.009	203.13 ± 0.014	195.97 ± 0.012
	r_F^2	0.9997	0.9996	0.9996
q_{exp} (mmol/g)		0.0947± 0.005	0.0923± 0.0037	0.0902± 0.0021

Table 3. Isotherm parameters for adsorption of radionuclides onto PMB*.

Adsorption isotherm and parameters		Temp. (°C)	Radionuclide		
			Cs(I)	**Co(II)**	**Eu(III)**
Freundlich	1/n	30	0.932 ± 0.0325	0.942 ± 0.029	0.973 ± 0.034
		40	0.929 ± 0.0302	0.937 ± 0.025	0.968 ± 0.031
		50	0.924 ± 0.284	0.934 ± 0.022	0.961 ± 0.299
	K_F	30	0.152 ± 0.0312	0.112 ± 0.0281	0.085 ± 0.0412
		40	0.177 ± 0.0494	0.136 ± 0.0404	0.099 ± 0.0293
		50	0.205 ± 0.0638	0.139 ± 0.0434	0.109 ± 0.0285
	r_F^2	30	0.9971	0.9975	0.9981
		40	0.9903	0.9935	0.9966
		50	0.9838	0.9924	0.9967
Langmuir	q_{max} (mmol/g)	30	0.732 ± 0.0089	0.644 ± 0.0035	0.555 ± 0.0023
		40	0.743 ± 0.0092	0.651 ± 0.0041	0.574 ± 0.0031
		50	0.752 ± 0.0097	0.667 ± 0.0049	0.583 ± 0.0037
	K_L (L/mmol)	30	0.358 ± 0.017	0.309 ± 0.0047	0.249 ± 0.012
		40	0.447 ± 0.021	0.381 ± 0.0055	0.307 ± 0.023
		50	0.534 ± 0.029	0.386 ± 0.0062	0.328 ± 0.027
	r_F^2	30	0.9989	0.9993	0.9993
		40	0.9958	0.9949	0.9934
		50	0.9957	0.9943	0.9937
q_{exp} (mmol/g)		30	0.691 ± 0.0071	0.603 ± 0.0032	0.518 ± 0.0018
		40	0.716 ± 0.0074	0.624 ± 0.0042	0.541 ± 0.0024
		50	0.737 ± 0.0082	0.647 ± 0.0053	0.561 ± 0.0033

*Conditions: PMB mass = 10 g/L; shaking time = 3h.

Plots of the two applied isotherm models, Eq. (3) and (4), obtained at the different temperatures studied were found to be linear (not shown). The fitting results of both Freundlich and Langmuir models are shown in Figure 6a-b, respectively, and all of the isotherm parameters, derived from the slope and intercept of the respective plots, are presented in Table 2. As seen in the table, the values of q_{max} and K_F derived from the Langmuir and Freundlich isotherms, respectively (which are related to the adsorption capacity) decreased with increase in temperature, indicating that the adsorption capacity of the dye is lowered at higher temperatures which implies that adsorption of C2B onto PMB is an exothermic process. When the r_F^2 and r_L^2 values (Table 2) are compared it can be concluded that the adsorption isotherms are better described by the Langmuir equation. Table 2 shows also that the monolayer saturation capacity of bentonite, q_{max}, at 30 °C is 0.0947 mmol C2B (~44.3 mg) per gram PMB.

3.5.2. Sorption of radionuclides

The sorption isotherms for simultaneous sorption of Cs(I), Co(II) and Eu(III) were obtained at three different temperatures 30, 40 and 50±1°C by varying the initial concentration of each radionuclide, in the solution to be treated, from 1x10^{-5} M to 2.8x10^{-2} M while keeping constant all other sorption conditions, i.e. sorbent weight 0.25 g, solution volume 25 mL, pH 7.3±0.1 and shaking time 3h. Data obtained were fitted to Freundlich (Eq. (3)) and Langmuir (Eq. (4)) adsorption isotherms and those achieved for Freundlich isotherm at 30 °C are displayed in Figure 6c. The parameters of the two applied isotherms were computed from the slope and intercept of the straight lines of the corresponding plots, and are given along with the correlation coefficients (r^2) in Table 3, which demonstrate that the present system can be explained well both by Freundlich and Langmuir adsorption isotherm models. Concerning the radionuclides sorption, it assumably occurs by exchange of the loosely bound ions, e.g. Na^+ and K^+, present between alumina and silica layers of non-modified bentonite with the radionuclide cations. As can be observed in Figure 6c, there is no significant difference between the log-log plots (Freundlich plots) for Cs, Co and Eu suggesting similar sorption mechanisms for the three radionuclides. The plots are linear with slope ($1/n$) very close to 1.0 (Table 3) up to ion concentration of about 1x10^{-2} M. At higher radionuclides concentrations, the plots show non-linearity (Figure 6c). These observations possibly indicate prevailing ion-exchange at concentrations < 1x10^{-2} M and presence of other types of sorption mechanisms, in addition to ion-exchange, at higher concentrations [31]. However Figure 6c reveals that the adsorption affinity for the radionuclides differs for the different cations. Thus the affinity decreases in the order Cs(I) > Co(II) > Eu(III). This sorption trend is contradictory to what is expected because the selectivity of the surface of an adsorbent is known to be greater for cations of the greater valency [39]. However, the preferential uptake of monovalent (Cs) to bivalent cation (Sr) was also reported by Bors *et al.* [28,32] and has been attributed to the lower hydration energy (larger ionic diameter) of Cs(I). By similar argument, decrease of sorption selectivity with increase of valency of radionuclide (Figure 6c) may be interpreted since the hydrated radii in nanometer of Cs(I) and Co(II) are 0.329 and 0.423 [39], respectively. That of Eu(III) is not available.

3.6. Thermodynamic parameters

From the sorption data at different temperatures, the enthalpy (ΔH^o), entropy (ΔS^o) and free energy of adsorption (ΔG^o) were calculated using the equations:

$$\ln K_L = \frac{\Delta S^o}{R} - \frac{\Delta H^o}{RT}, \qquad (5)$$

Table 4. Thermodynamic parameters for adsorption of C2B onto PMB.

Temp. (°C)	ΔG° (kJ mol⁻¹)	ΔH° (kJ mol⁻¹)	ΔS° (kJ mol⁻¹K⁻¹)
30	-13.662±0.023	-5.845 ± 0.527	0.0258 ± 0.0025
40	-13.924±0.038		
50	-14.178±0.032		

Table 5. Thermodynamic parameters for adsorption of radionuclides onto PMB*.

Radionuclide	Temp. (°C)	ΔG° (kJ mol⁻¹)	ΔH° (kJ mol⁻¹)	ΔS° (kJ mol⁻¹K⁻¹)
Cs(I)	30	2.588±0.0779	16.625 ± 0.553	0.04633 ± 0.0038
	40	2.095±0.0546		
	50	1.685±0.0428		
Co(II)	30	2.958±0.0156	11.409 ± 0.522	0.0279 ± 0.0029
	40	2.589±0.0143		
	50	2.422±0.0126		
Eu(III)	30	3.502±0.0681	10.521 ± 0.645	0.02553 ± 0.0025
	40	3.152±0.0598		
	50	2.993±0.0322		

*Conditions: PMB mass = 10g/L; shaking time = 3h

$$\Delta G^o = -RT\ lnK_L \tag{6}$$

Where R (J/mol.K) is the universal gas constant, T is the absolute temperature, and K_L is the Langmuir constant related to the intensity of adsorption (L/mmol). The ΔH^o and ΔS^o values were calculated from the slope and y-intercept of the plot of $\ln K_L$ vs. 1/T, respectively (Figure 7).

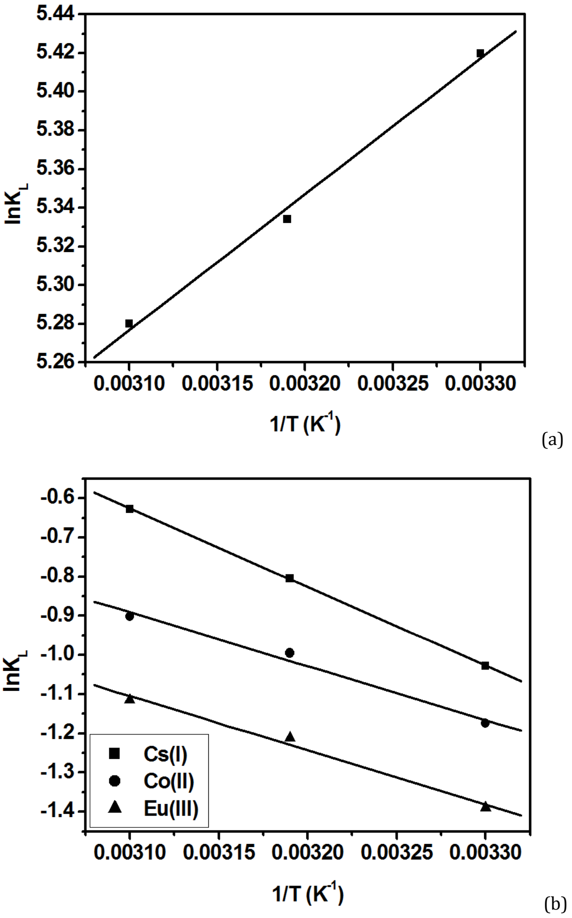

Figure 7. Plots of $\ln K_L$ vs. 1/T for sorption of C2B (a) and radionuclides (b) onto PMB.

3.6.1. Thermodynamic parameters of C2B

The ΔG^o values for C2B are given together with the values of ΔH^o and ΔS^o in Table 4 which shows a negative value of the enthalpy change, ΔH^o. This indicates that decrease of temperature favored adsorption of C2B onto PMB, that is the interaction between the dye and organoclay is exothermic. The positive value of ΔS^o suggests increased randomness at the solid/solution interface during the adsorption process.

Generally, the magnitude of the change in Free energy, ΔG^o, can give information whether adsorption takes place by a physical or a chemical process. According to literature [40], if ΔG^o ranges between 0 and -20 kJ/mol, the adsorption process is of a physical nature, but if it ranges between -80 and -400 kJ/mol, the adsorption process is a chemical one. Hence, the numerical negative values of ΔG^o (Table 4) obtained under the experimental conditions, indicate that adsorption of C2B by PMB is a physisorption process which is consistent with the foregoing deduction that electrostatic and hydrophobic attractions are involved in the adsorption process. The negative sign of the sorption process at all the test temperatures indicates the feasibility of the process and its spontaneous nature. The shift of the magnitude of the standard free energy to more negative values with temperature increases from 30 to 50 °C suggests that the adsorption process is more spontaneous at high temperatures.

3.6.2. Thermodynamic parameters of radionuclides

The values of thermodynamic parameters listed in Table 5 show that sorption of Cs(I), Co(II) and Eu(III) on PMB is an endothermic process. The positive value of ΔH^o shows that the reaction is more favorable at higher temperatures. As reported by Khan *et al.* [41] the positive value of ΔS^o suggests that the adsorbed cations are relatively immobile and the ions displaced from the solid surface are greater in number than the adsorbed ions; e.g. two monovalent cations may be displaced from the adsorbent surface for one Co(II) ion adsorbed.

3.7. Kinetic studies

To determine the kinetic parameters for practical application of the adsorption process, the kinetic data has been treated by pseudo-first-order (Lagergren rate equation) [42] and pseudo-second-order kinetic models [43]; Eq. (7) and (8), respectively:

$$ln(q_e - q_t) = ln\, q_{e1} - k_1 t \tag{7}$$

$$\frac{t}{q_t} = \left(\frac{1}{k_2\, q_{e2}^2}\right) + \left(\frac{t}{q_{e2}}\right) \tag{8}$$

where q_e and q_t are the amount of solute sorbed onto PMB (mmol/g) at equilibrium and at time t, respectively. k_1 and k_2 are pseudo-first-order and pseudo-second-order rate constants, respectively.

Table 6. Kinetic parameters for adsorption of C2B (A) onto PMB.

Kinetic model and parameters		Initial C2B concentration (C_o), mmol L^{-1}			
		C_o = 0.1	C_o = 0.2	C_o = 0.4	C_o = 0.6
Pseudo-first-order	k_1	0.6866 ± 0.0127	0.3988 ± 0.0105	0.3107 ± 0.0151	0.2675 ± 0.0091
	q_{e1} (mmol g^{-1})	0.0099 ± 0.0004	0.0209 ± 0.0009	0.0419 ± 0.0034	0.0545 ± 0.0035
	r^2	0.9991	0.9972	0.9918	0.9949
Pseudo-second-order	k_2	73.82 ± 1.5243	11.3 ± 0.2764	1.442 ± 0.01389	0.428 ± 0.00321
	q_{e2} (mmol g^{-1})	0.0114 ± 0.0007	0.0255 ± 0.0009	0.0654 ± 0.0051	0.1118 ± 0.0178
	r^2	0.9881	0.9944	0.9716	0.8687
q_{exp} (mmol g^{-1})		0.0099± 0.0002	0.0190± 0.0005	0.0335± 0.0025	0.0415± 0.0045

Table 7. Kinetic parameters for adsorption of radionuclides onto PMB.

Kinetic model and parameters		Cs(I)	Co(II)	Eu(III)
Pseudo-first-order	k_1	0.0252 ± 0.00079	0.0331 ± 0.0012	0.051 ± 0.001
	q_{e1} (mmol g^{-1})	0.00848 ± 0.0007	0.0077 ± 0.0006	0.0066 ± 0.0005
	r^2	0.9941	0.9936	0.9964
Pseudo-second-order	k_2	0.1551 ± 0.0073	1.168 ± 0.041	2.695 ± 0.065
	q_{e2} (mmol g^{-1})	0.0238 ± 0.0045	0.0111 ± 0.0031	0.0093 ± 0.0007
	r^2	0.9831	0.9851	0.9897
q_{exp} (mmol g^{-1})		0.00714± 0.0005	0.00637± 0.00035	0.00568± 0.00025

Conditions: radionuclide conc. = $1x10^{-6}$ M; temp. = 30±1°C; PMB mass = 10 g/L.

3.7.1. Sorption kinetics of C2B

Linear plots of ln (q_e – q_t) versus t (Eq. 7) and of t/q_t versus t (Eq. 8) for different initial C2B concentrations were obtained (not shown). From the slope and intercept of the corresponding plot the value of K_1, K_2, q_{e1} and q_{e2} were determined and are listed in Table 6. In the same table are given, for comparison, the experimental values of q_e (q_{exp}). As seen from the data in the Table 6, the correlation coefficients for the pseudo-first-order kinetic plots at the different studied dye concentrations are all above 0.992 and higher than those of the second-order equation. Also, the calculated q_{e1} values are generally much closer to the q_{exp} values compared to the calculated q_{e2} values. These results imply that the present adsorption system obeys the pseudo-first-order rate equation.

The variation in the dye quantity adsorbed with the contact time at various initial dye concentrations was then processed using the intraparticle diffusion model (Eq. 9) [44] to evaluate the role of diffusion in the adsorption process:

$$q_t = k_i t^{1/2} + C \qquad (9)$$

Where q_t is the amount of solute (C2B) adsorbed (mmol/g) at time t, k_i is the intraparticle rate constant (mmol g^{-1} $min^{-1/2}$). If intraparticle diffusion is rate controlling, the plots are linear and passing through the origin [44]. On the other hand, if the plots are linear but do not pass through the origin the rate of adsorption may be controlled by intraparticle diffusion together with other kinetic models.

Figure 8a shows plots of q_t versus $t^{1/2}$ for the effect of initial dye concentration on the dye adsorption. As observed, the plots do not pass through the origin indicating that intraparticle diffusion is involved in the sorption process but it is not the sole rate-controlling mechanism. Also, the plots show multilinearity which implies that the sorption process involves more than one step. Each plot has three different portions: an initial curve portion, followed by a linear portion and a plateau. The initial portion can be attributed to surface adsorption and rapid external diffusion that is boundary layer diffusion (film diffusion).

The second linear portion is the gradual adsorption stage where the intraparticle diffusion predominates. The plateau region is the final equilibrium stage, where the intraparticle diffusion starts to slow down due to the low solute concentration in solution [45].

3.7.2. Sorption kinetics of radionuclides

The sorption rate data obtained for simultaneous sorption of the three concerned radionuclides were treated as pseudo-first-order rate and pseudo-second-order rate equation. Straight line plots were obtained from which the rate parameters were derived and are listed in Table 7 along with the correlation coefficients (r^2). As shown from the table, the r^2 values for the pseudo-first-order kinetic plots for the three studied radionuclides are higher than those of the second-order-kinetic model, and the calculated q_{e1} values agree with the experimental sorption capacity values (q_{exp}) indicating that the sorption of the radionuclides follows the first-order rate equation. As it is the case of C2B sorption, plots of q_t versus $t^{1/2}$ (Eq. 9) for the radionuclides studied (Figure 8b) show that the sorption process is controlled by intraparticle diffusion and boundary layer diffusion.

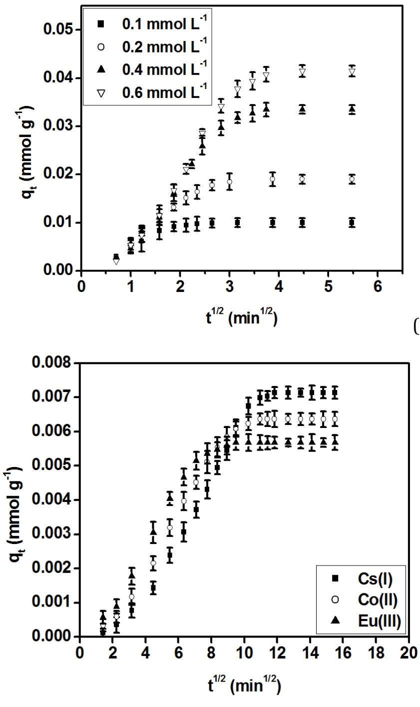

(a)

(b)

Figure 8. Amount of sorbate sorbed versus $t^{1/2}$ for intraparticle diffusion of C2B (a) and radionuclides (b) by PMB. Conditions: C2B conc. = $1x10^{-4}$ M; Radionuclide conc. = $1x10^{-6}$ M; PMB mass = 10 g/L; Temp. = 30 ± 1 °C.

Table 5: Results obtained for simultaneous removal of C2B and radionuclides from tap water and MRPWW *.

Adsorbate	Removal with 40g L^{-1} PMB from				Removal from MRPWW			
	(A) Tap water		(B) Tap water + 2 μg L^{-1} Zn^{2+}		(C) 40 g L^{-1} PMB		(D) 50 g L^{-1} PMB	
	R%	K_d**	R%	K_d**	R%	K_d**	R%	K_d**
C2B	99.92	124900	99.93	142757	99.91	111000	99.93	142757
^{137}Cs(I)	99.27	13598	99.25	13233	97.85	4551	99. 31	14393
^{60}Co(II)	99.21	12558	99.17	11948	96.97	3200	99.25	13233
$^{152+154}$Eu(III)	99.15	11664	99.12	11264	96.32	2617	99.19	12246

* Conditions: Initial C2B conc. = 1x10^{-4} M; initial radionuclide conc. = 1x10^{-6} M of each; shaking time = 3 h; temp. = 30±1 °C.

$$** \; K_d \,(\text{Distribution coefficient}) = \frac{\text{initial sorbate conc.} - \text{final sorbate conc.}}{\text{final sorbate conc.}} \, x \, \frac{volume\ of\ solution\ (mL)}{weight\ of\ sorbent\ (g)}$$

3.8. Potential use of PMB to treat MRPWW

As apparent from Figure 5a the dye has a strong affinity for adsorption onto PMB over a fairly wide range of pH values, but successful sorption of radionuclides is limited to pH values >9.5 (Figure 5b). Due to the nearly neutral pH of RPWW(s), it has been necessary to extend the pH range of successful removal towards the acidic side so as to avoid adjustment of the pH of the wastewater to be treated. In an attempt to achieve this target the effect of the adsorbent dosage on the efficiency of removal of the radionuclides at neutral pH was studied by varying the mass of the adsorbent from 0.2 to 1.6 g/25 mL of solution 1x10^{-6} M in each of Cs(I), Co(II) and Eu(III). The results revealed that the percentage adsorptions increase markedly with increasing amount of the adsorbent up to 0.8 g/25 mL (32 g/L) where removals approaching 100% are achieved. Therefore, unless otherwise stated, adsorbent mass of 1 g/ 25 mL (40 g/L) was selected for the following experiments.

The effectiveness of the developed process for simultaneous removal of C2B and the radionuclides from tap water and for treatment of the simulated C2B-containing radioactive process wastewater (MRPWW) (Table 1) was then tested.

As shown from the results (Table 8) almost complete removal of the dye was achieved from both tap water and MRPWW. Concerning the radionuclides, removals exceeding 99% were achieved from tap water (Table 8, column A), but the removal efficiency was decreased when MRPWW was used (Table 8, column C) under similar experimental conditions of pH and adsorbent weight, 1 g/ 25 mL (40 g/L). As can be observed (Table 8, columns A and D) there is no significant difference in sorption efficiency between the monovalent Cs(I), divalent Co(II) and trivalent Eu(III) metal cations. This observation suggests similar sorption mechanism. Hence, reduction in percentage removal of the radionuclides from MRPWW as compared to tap water is unlikely caused by precipitation or complex formation with any of the compounds present in the wastewater. This difference in removal efficiency may be, therefore, attributed to presence in the MRPWW of other metal cations (Zn(II) in the present case) in addition to the radionuclides and/or to the presence of organic compounds. As shown from the results obtained for tap water (Table 8), the removal efficiency was not significantly affected by presence of Zn(II) in concentration similar to that in MRPWW. Consequently, reduction in the efficiency of removal of the radionuclides from MRPWW as compared to tap water seems to be caused by the presence of organic extractants. A possible explanation for extractants effect may be found in work published by Zhu *et al.* [46]. Their results suggest that at low concentrations sorption of some organics, which ordinarily sorb to CTAB-bentonite by partition, appeared to result significantly from adsorption or other specific interaction in addition to partition. The reason for this behaviour was ascribed [46] to presumed low partition of those organics caused by large disparity in their polarity and the nonpolar CTAB medium. For a similar reason, sorption of organics present in the MRPWW may be partly due to adsorption, thereby occupying vacant sorption sites. As a result, adsorption of metal cations (radionuclides) decreased due to reduction in the number of available sorption sites. In support to this hypothesis is the finding that high removal values could be maintained by increasing the PMB/liquid ratio (Table 8, column D), which governs the supply of available sorption sites.

4. Conclusions

Bentonite partially modified (PMB) with cetyltrimethyammonium bromide (CTAB) renders the clay capable to simultaneously adsorb the anionic chemically toxic pollutant C2B and the cationic radionuclides ^{137}Cs(I), ^{60}Co(II) and $^{152+154}$Eu(III) from aqueous solutions. Removal of C2B singly and of the radionuclides simultaneously from aqueous solutions were studied in detail. Almost complete removal of C2B is achieved over a wide range of pH (2.5-12.7) while quantitative sorption of radionuclides can only be achieved at about pH = 7 and above. C2B loadings as high as 0.0947 mmol/g PMB (~44 mg/g) is achieved at 30 °C. Langmuir model is more appropriate for describing the sorption equilibrium data, of both C2B and the radionuclides, than Freundlich model. The monolayer coverage of PMB by ^{137}Cs(I), ^{60}Co(II) and $^{152+154}$Eu(III) are 0.732, 0.644 and 0.555 mmol/g PMB, respectively. Electrostatic attraction and hydrophobic interaction are suggested to be the dominant interaction between C2B and PMB. Ion-exchange appears to be the principal sorption mechanism for radionuclides at concentrations below about 1x10^{-2} M. At higher concentrations other sorption mechanisms seem to take place in addition to ion-exchange. Isotherms at different temperatures and thermodynamic calculations indicate that adsorption of C2B is an exothermic process while sorption of the radionuclides is an endothermic one. The negative values of free energy change for C2B indicate the spontaneous nature of sorption. The sorption kinetics both for C2B and the radionuclides follow pseudo-first-order model and the sorption process appears to proceed by external surface adsorption and intraparticle diffusion.

Under the optimal conditions for simultaneous sorption of the pollutants from MRPWW, which are mainly determined by the sorbent dosage and the initial pH (has to be ≥7), removals approaching 100% and >99% are achieved for C2B and for each of the tested radionuclides, respectively.

References

[1]. Shakir, K.; Aziz, M.; Salama, H. N.; Benyamin, K. *Radiochimica Acta* **1987**, *41*, 47-53.

[2]. Shakir, K.; Elkafrawy, A. F.; Ghoneimy, H. F.; Beheir, Sh. G.; Refaat, M. *Water Res.* **2010**, *44*, 1449-1461.

[3]. Shakir, K.; Aziz, M. *Radiochemica Acta* **1979**, *26*, 113-116.

[4]. Omar, H. A.; Aziz, M.; Shakir, K. *Radiochim. Acta* **2006**, *94*, 1–8.

[5]. Shakir, K.; Ghoneimy, H. F.; Beheir, Sh. G.; Refaat, M. *Sep. Sci. Technol.* **2007**, *42*, 1341–1365.

[6]. Shakir, K.; Sohsah, M.; Soliman, M. *Sep. Purif. Technol.* **2007**, *54*, 373-381.

[7]. Snell, F. D. Photometric and fluorometric methods of analysis, Part 2; John Wiley and Sons, New York, 1978.

[8]. Vaghela, S. S.; Jethva, A. D.; Mehta, B. B.; Dave, S. P.; Adimurthy, S.; Ramachandraiah, G. *Environ. Sci. Technol.* **2005**, *39*, 2848–2855.

[9]. Sangal, S. P. *Microchem. J.* **1964**, *8*, 313-316.

[10]. Sangal, S. P. *Bull. Chem. Soc. Japan* **1965**, *38*, 141-142.

[11]. Abdel-Ghani, N. T.; Shoukry, A. F.; Issa, Y. M.; Wahdan, O. A. *J. Pharm. and Biomed. Anal.* **2002**, *28*, 373-378.

[12]. Qamar, M.; Saquib, M.; Muneer, M. *Dyes Pigm.* **2005***, 65*, 1-9.

[13]. Sax, N. I. (Ed.) Cancer causing chemicals; VNR, New York, 1981.

[14]. Song, S.; Ying, H.; He, Z.; Chen, J. *Chemosphere* **2007**, *66*, 1782–1788.

[15]. Wei, J.; Zhu, R.; Zhu, J.; Ge, F.; Yuan, P.; He, H.; Ming, C. *J. Hazard. Mater.* **2009**, *166*, 195-199.

[16]. Kubilay, S.; Gürkan, R.; Savran, A.; Sahan, T. *Adsorption* **2007**, *13*, 41-51.

[17]. Sabodina, M. N.; Kalmykov, S. N.; Sapozhnikov, Y. A.; Zakharova, E. V. *J. Radioanal. Nucl. Chem.* **2006**, *270*, 349-355.

[18]. Stumm, W.; Morgan, J. J. Aquatic Chemistry, an International Emphasizing Chemical Equilibria in Natural Waters, John Wiley & Sons, New York, 1981.

[19]. Hendricks, S. B.; Jefferson, M. E. *Am. Mineral.* **1938**, *23*, 863–875.

[20]. Xu, S. H.; Boyd, S. A. *Environ. Sci. Technol.* **1995**, *29*, 313–320.

[21]. Kwolek, T.; Hodorowicz, M.; Stadnicka, K.; Czapkiewicz, J. *J. Coll. Inter. Sci.* **2003**, *264*, 14–19.

[22]. Abate, G.; Santos, L. B. O.; Colombo, S. M.; Masini, J. C. *Appl. Clay Sci.* **2006**, *32*, 261–270.

[23]. Anirudhan, T. S.; Ramachandran, M. *J. Coll. Inter. Sci.* **2006**, *299*, 116–124.

[24]. Dultz, S.; Bors, J. *Appl. Clay Sci.* **2000**, *16*, 15–29.

[25]. Shakir, K.; Ghoneimy, H. F.; Elkafrawy, A. F.; Beheir, Sh. G.; Refaat, M. *J. Hazard. Mater. B* **2008**, *150*, 765-773.

[26]. Wang, M. K.; Wang, S. L.; Wang, W. M. *Soil Sci. Soc. Am. J.* **1996**, *60*, 138-141.

[27]. Rosen, M. J.; Goldsmith, H. A. Systematic analysis of surface-active agents, 2nd Ed., John Wiley & Sons, Inc., New York, 1972.

[28]. Bors, J.; Dultz, St.; Riebe, B. *Eng. Geology* **1999**, *54*, 195–206.

[29]. Jaynes, W. F.; Boyd, S. A. *Soil Sci. Soc. Am. J.* **1991**, *55*, 43-48.

[30]. Madejová, J. *Vib. Spectrosc.* 2003, *31*, 1-10.

[31]. Bors, J.; Dultz, St.; Riebe, B. *App. Clay Sci.* **2000**, *16*, 1-13.

[32]. Bors, J.; Dultz, St.; Gorny, A. *Radiochim. Acta* **1998**, *82*, 269–274.

[33]. Khalifa, H.; Khater, M. A.; El-Sirafy, A. A. *Fres. J. Anal. Chem.* **1968**, *237*, 111-117.

[34]. Stumm, W. Chemistry of the solid-water interface; John Wiley & Sons, New York, 1992.

[35]. Parks, G. A. *Chem. Rev.* **1965**, *65*, 177-198.

[36]. Zohra, B.; Aicha, K.; Fatima, S.; Nourredine, B.; Zoubir, D. *Chem. Eng. J.* **2008**, *136*, 295-305.

[37]. Chiou, M. S.; Li, H. Y. *Chemosphere* **2003**, *50*, 1095-1105.

[38]. Wang, J.; Somasundran, P.; Nagaraj, D. R. *Miner. Eng.* **2005**, 18, 77-81.

[39]. Essington, M. E. Soil and water chemistry: An introductive approach, CRC Press, New York, 2004.

[40]. Petrucci, R. H.; Harwood, W. S. General Chemistry: Principles and Modern Applications, 7th ed., Prentice Hall, New Jersey, 1997.

[41]. Khan, S. A.; Reman, R.; Khan, M. A. *J. Radioanal. Nucl. Chem.* **1995**, *190*, 81-96.

[42]. Lagergren, S. *Handlingar* **1898***, 24,* 1-39.

[43]. Ho, Y. S.; McKay, G. *Process Biochem.* **1999***, 34*, 451-465.

[44]. Weber, W. J.; Morriss, J. C. *J. Sanitary Eng. Div. Am. Soc. Civ. Eng.* **1963**, *89*, 31-51.

[45]. Crini, G.; Peindy, H. N.; Gimbert, F.; Robert, C. *Sep. Purif. Technol.* **2007**, *53*, 97-110.

[46]. Zhu, L. Z.; Ren, X.; Yu, H. *Environ. Sci. Technol.* **1998**, *32,* 3374-3378.